Electronic Supplementary Information

Structure and EPR Characterization of N,N’-bis(5-tert-butylsalicylidene)-1,2-Cyclohexanediamino-Vanadium (IV) Oxide and its adducts with propylene oxide

E. Carter,[a] I. A. Fallis,[a] B. M. Kariuki,[a] I.R. Morgan,[a] D. M. Murphy,[a] T. Tatchell,[a]
S. Van Doorslaer[b], E. Vinck[b]

[a] *School of Chemistry, Cardiff University, Main Building, Park Place,*
Cardiff, CF10 3AT, UK.

[b] *SIBAC laboratory – Department of Physics, University of Antwerp,*
Universiteitsplein 1, B-2610 Wilrijk, Belgium.

CONTENTS

Figure S1	Experimental (solid) and simulated (dashed) CW-ENDOR [10K] of *rac*-[VO(**3**)] dissolved in dichloromethane/ toluene recorded at the magnetic field positions corresponding to a) $g_{\|}$, b) $g_{\perp}$ and c) g_{iso}.
Figure S2	Experimental (solid) and simulated (dashed) cw- ^{1}H ENDOR spectra of *R,R’*-[VO(**3**)] dissolved in *S*-(**4**), recorded at the field positions corresponding to a) $g_{\|}$, b) $g_{\perp}$ and c) g_{iso}.
Figure S3	Simulated MIMS ENDOR spectra for varying *tau* values.
Scheme S1	Schematic illustration of the binding mode of the epoxide to [VO(**3**)] based on the information extracted from the ENDOR spectra.
Figure S4	Evaluation, analysis and explanation of the HYSCORE data.
Figures S5/S6	Calculated ground state and spin-density distribution of [VO(**3**)].
Figure S7	DFT calculated atomic coordinates of [VO(**3**)], optimized using BP86/SVP for all atoms, excluding V for which TZV_PP is used.
Table S1	DFT calculated coordinates for [VO(**3**)]

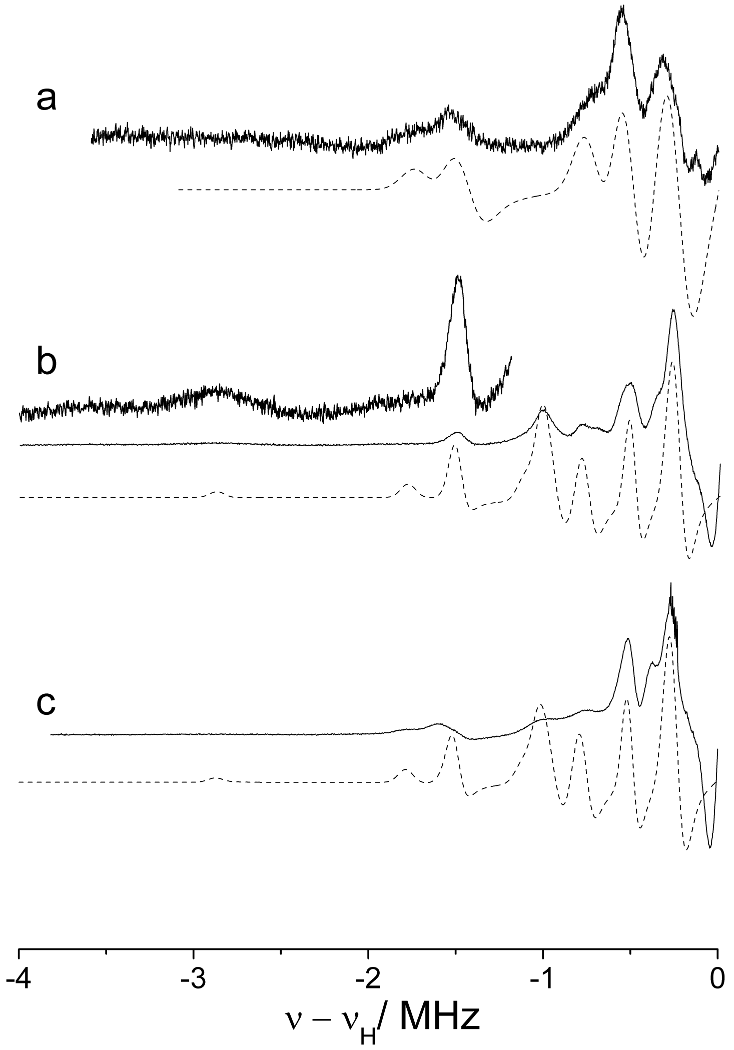

Figure S1 Experimental (solid) and simulated (dashed) cw ^{1}H-ENDOR of *R,R'*-[VO(**3**)] in tol/ DCM recorded at the field positions corresponding to a) $g_{\parallel}$, b) $g_{\perp}$ and c) g_{iso}.

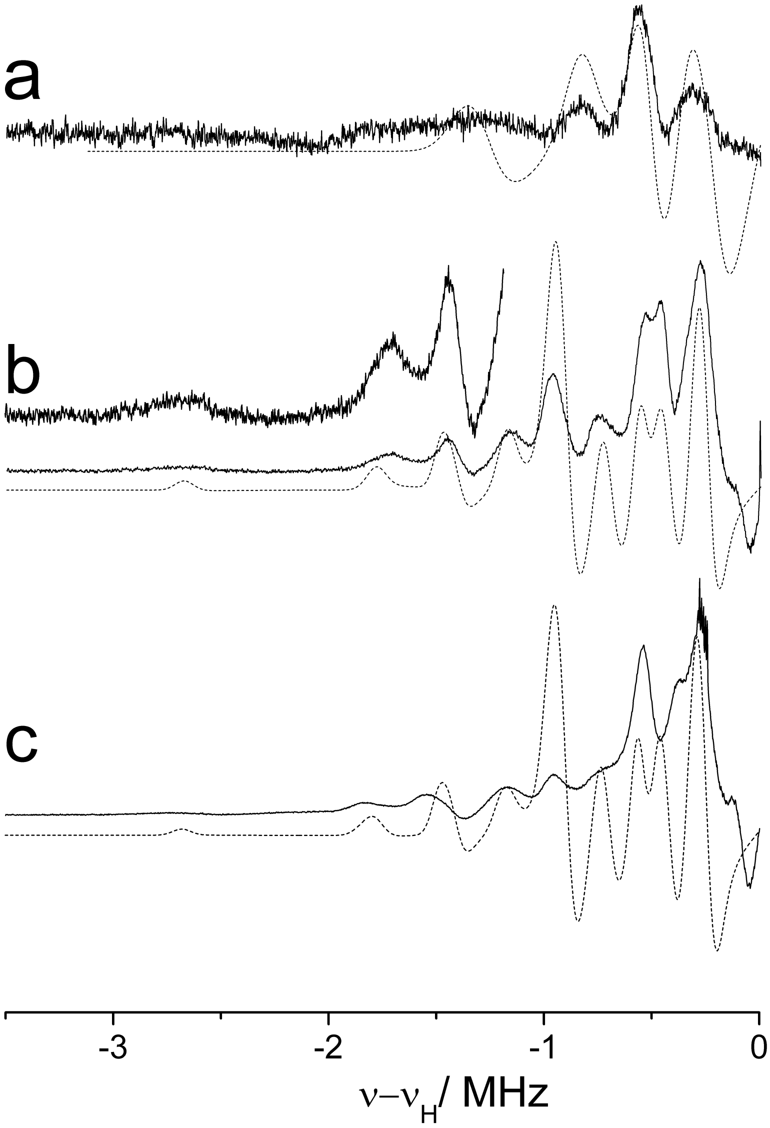

Figure S2 Experimental (solid) and simulated (dashed) cw- ^{1}H ENDOR spectra of *R*,*R'*-[VO(**3**)] dissolved in *S*-(**4**), recorded at the field positions corresponding to a) $g_{\parallel}$, b) $g_{\perp}$ and c) g_{iso}.

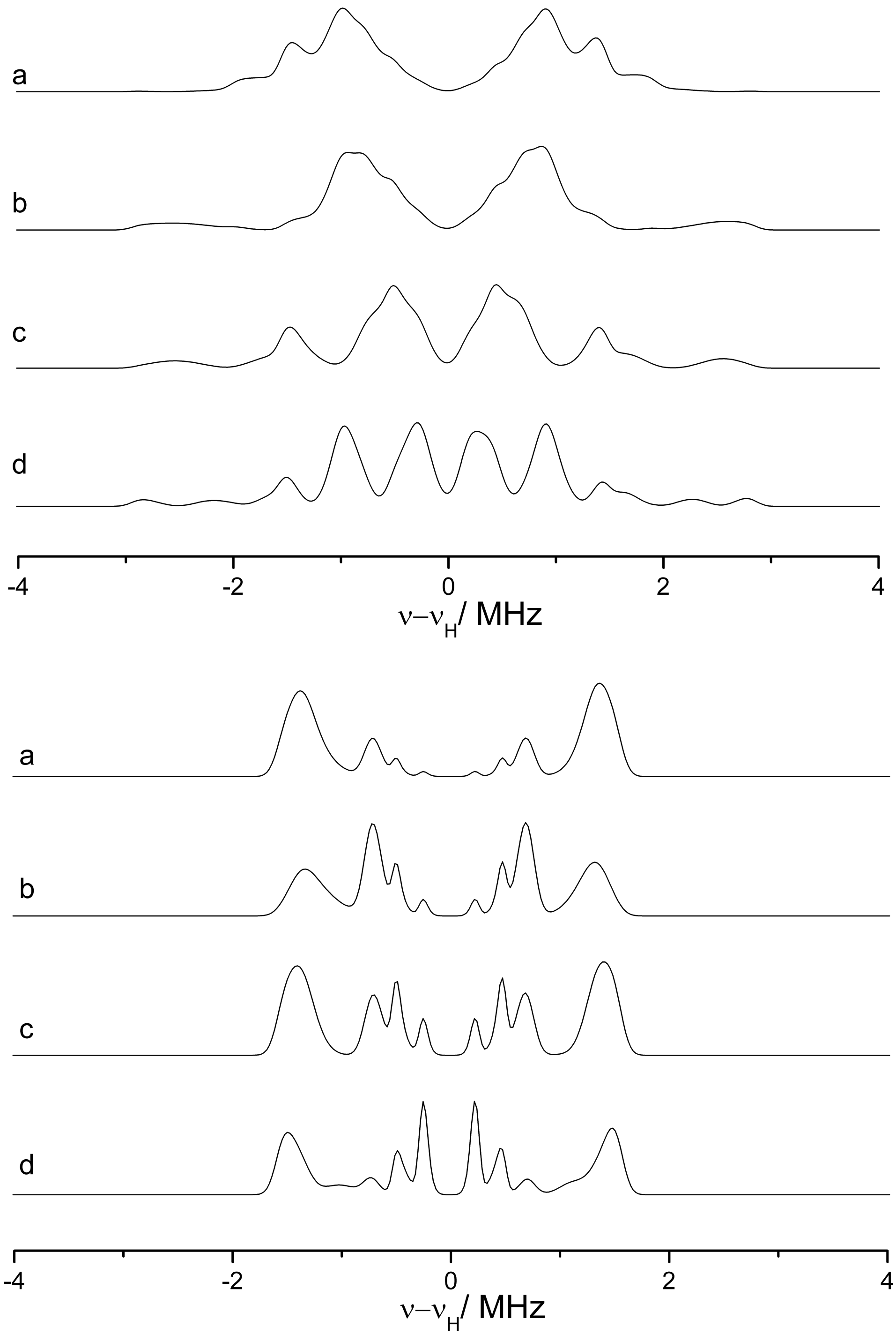

Figure S3 Simulated Mims ^{1}H-ENDOR of [VO(**3**)] recorded at the field positions corresponding to (top) $g_{\perp}$ and (bottom) $g_{\parallel}$. The pulse sequence $\pi/2_{\mathrm{MW}}$-τ-$\pi/2_{\mathrm{MW}}$-π_{RF} - $\pi/2_{\mathrm{MW}}$-τ-echo was used assuming infinitely short pulse lengths and an interpulse delay time τ of a) 192 ns, b) 292 ns, c) 492 ns and d) 792 ns. Simulations performed using EASYSPIN.

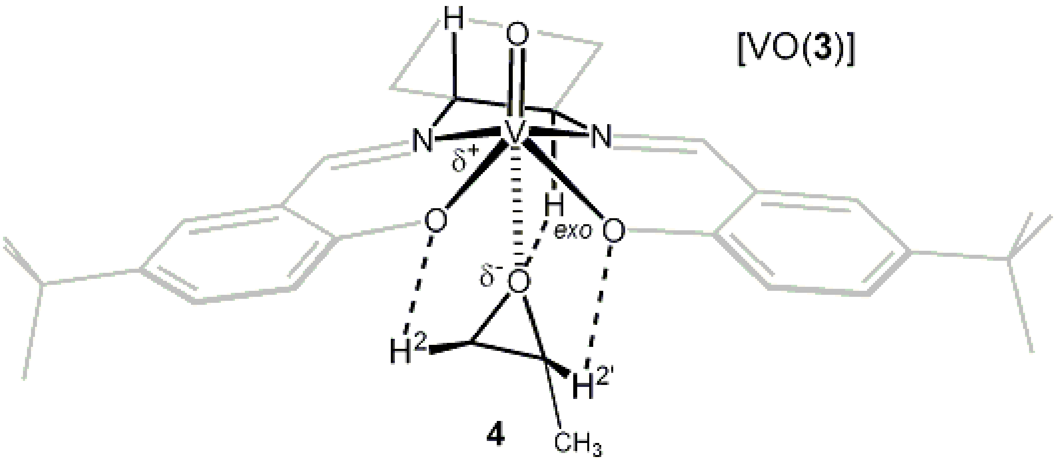

Scheme S1 Schematic illustration of the epoxide coordination mode based on the information extracted by analysis of the epoxide proton hyperfine data (which in turn was extracted by simulation of the ENDOR spectra).

Evaluation and analysis of the HYSCORE spectra

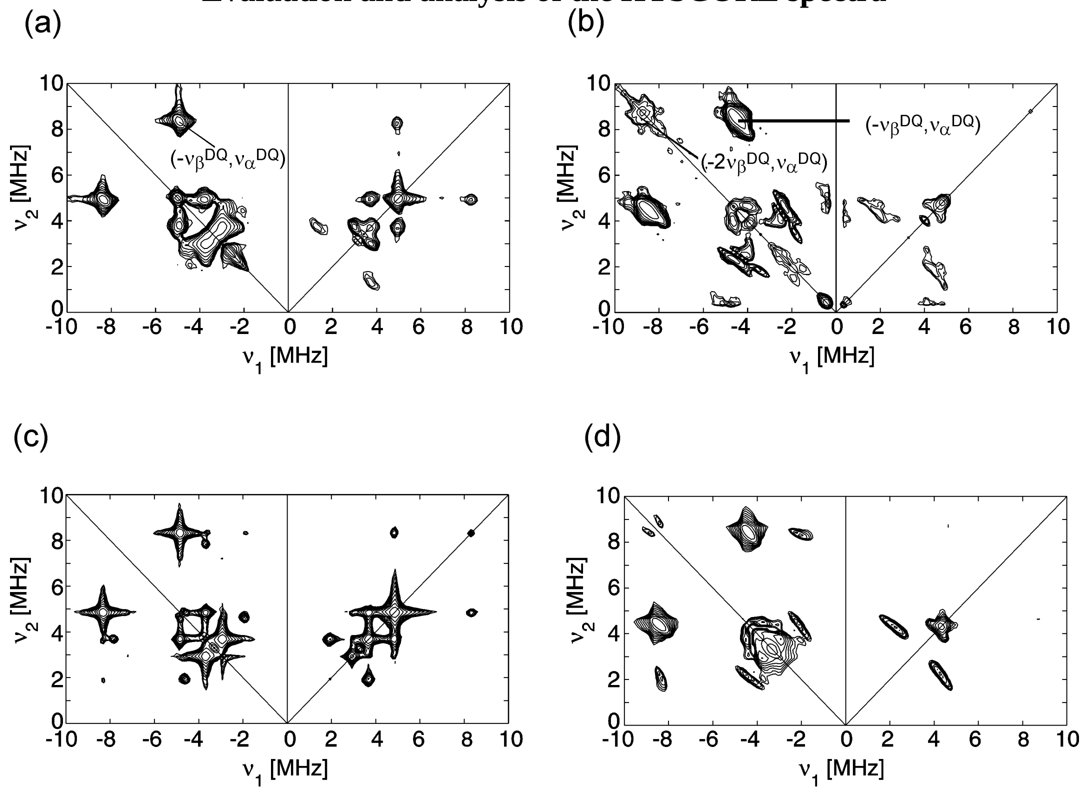

Figure S4: Enlargement of **Figure 5** in full text.

In the experimental HYSCORE spectra (S4a,b), strong cross peaks are observed in the (-,+) quadrant at approximately (-8, 5) MHz and (-5,8) MHz. These peaks correspond to the cross peaks between the double-quantum (DQ) nuclear transitions ($\Delta M_I=\pm2$) in both M_S manifolds. The DQ cross peaks are the strongest peaks in the spectrum because of two reasons: (a) the nuclear-quadrupole, hyperfine and nuclear Zeeman interaction are close in magnitude, which causes a high transition probability for the $\Delta M_I=\pm2$ transitions and (b) the double-quantum nuclear frequencies depend only in second order on the nuclear quadrupole interaction. The cross peaks in the [-6 - 6, 0 - 6] MHz area are cross peaks between two single-quantum (SQ) nuclear frequencies or SQ and DQ frequencies. The appearance of the DQ correlation peaks in the (-,+) quadrant indicates that the hyperfine value is larger than twice the nuclear Zeeman interaction (strong coupling case) and an initial guess of the hyperfine values and nuclear quadrupole values can be obtained using the approximate expression

$$\nu_{\alpha,\beta}^{DQ} = 2\sqrt{(\frac{a}{2} \pm \nu_I)^2 + K^2(3+\eta^2)}$$

with a the hyperfine value, ν_I the Larmor frequency, η the asymmetry parameter of the nuclear quadrupole value and the nuclear quadrupole coupling constant

$$K = \frac{e^2qQ}{4h}$$

The initial guess of the hyperfine and nuclear quadrupole couplings thus obtained can then be used as starting poit for the simulation of the HYSCORE spectra. In the current case, satisfactory fits could be obtained using the spin-Hamiltonian parameters found previously for [VO(**1**)] as explained in the main text.

Ground state and spin-density distribution of [VO(3)]

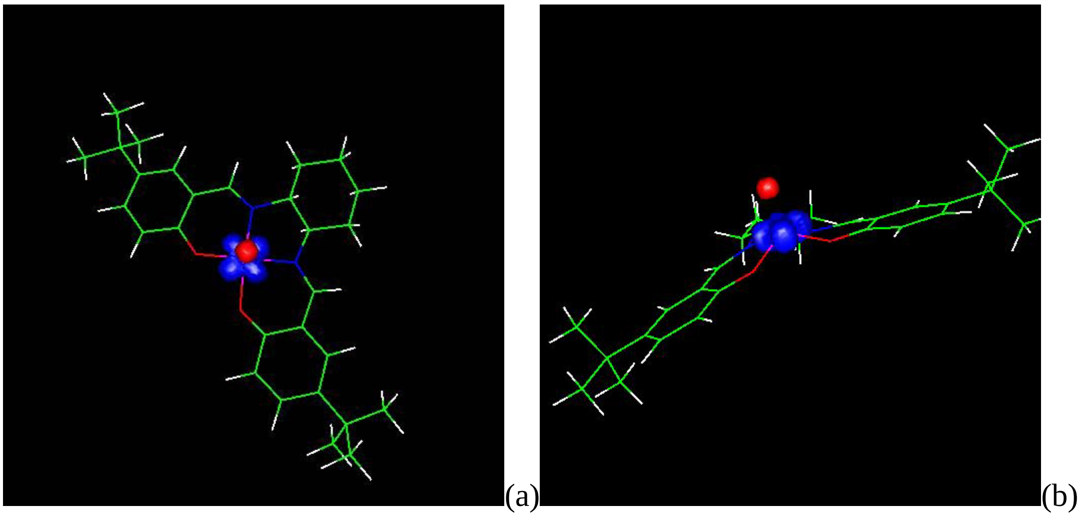
(a) (b)

Figure S5. Spin density distribution in [VO(**3**)]: top view (a) and side view (b). Blue: positive spin density, red: negative spin density. Contour lines -0.015 and 0.015.

From Figure S5, it is clear that the unpaired electron resides mainly in the d_{xy} orbital agreeing with the standard description of the ground state configuration of vanadyl centers as $(d_{xy})^1$. The Mulliken spin analyses gives a positive spin of 0.910953 for the V dxy orbital and an overall negative spin of -0.130963 in the p orbitals of the vanadyl oxygen. When the contours are lowered in the spin density distribution (Figure S6), we notice the negative spin density on the N of the ligand (**3**). Figure S5b shows that the H_{exo} and H_{endo} protons are clearly out of the xy plane, explaining the negligible spin density on these protons.

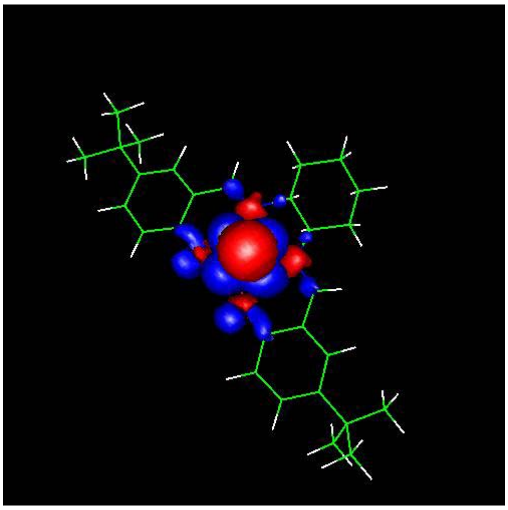

Figure S6. pin density distribution in [VO(**3**)]. Blue: positive spin density, red: negative spin density. Contour lines -0.0005 and 0.0005.

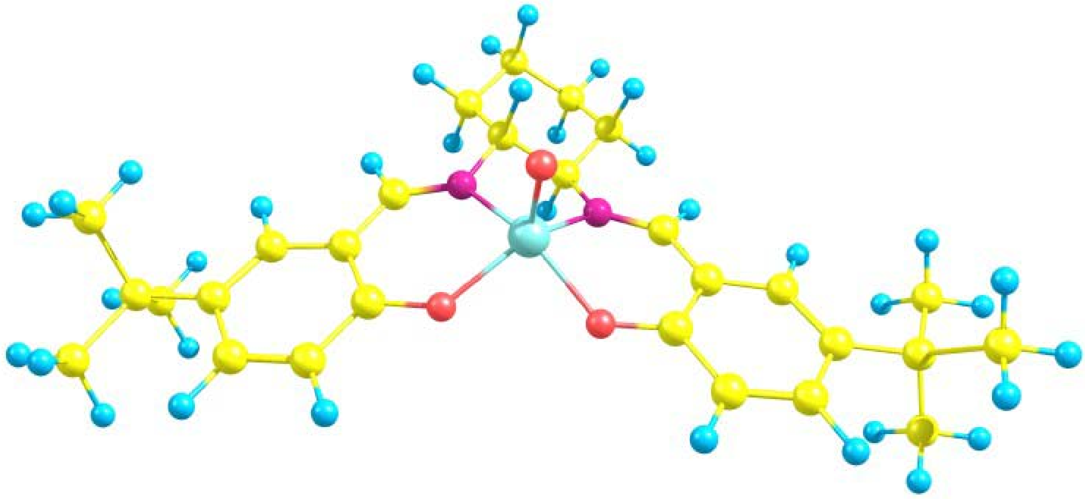

Figure S7 DFT calculated atomic coordinates of [VO(**3**)], optimized using BP86/SVP for all atoms, excluding V for which TZV_PP is used.

Table S1 DFT calculated coordinates for [VO(**3**)]

Atom	x	y	z
H	-2.400821	4.318544	-0.288565
H	1.830514	4.596915	-0.077761
H	-0.531361	5.855213	0.276676
H	1.130324	6.571665	-1.445710
H	-3.042635	2.375669	-0.973391
H	-0.291712	3.328106	0.635227
H	-8.203701	-2.531766	-1.731384
H	-6.305578	-0.976295	-3.648317
H	-7.919537	-0.446993	-3.064046
H	-6.494667	0.615118	-2.847182
H	-7.158764	-0.804177	0.641164
H	-8.418652	-0.345691	-0.554269
H	-7.001776	0.717367	-0.291116
H	-4.905513	1.082679	-1.231672
H	7.572615	2.068926	-0.297919
H	7.798585	0.107842	1.353857
H	7.899509	-1.577185	0.754390
C	-7.326511	-0.341259	-0.353050
C	-6.565533	-1.113123	-1.461461
C	-5.050091	-1.083013	-1.160693
C	-4.363637	0.134265	-1.078032
C	-2.971572	0.222117	-0.795322
C	-2.202344	-0.981802	-0.589367
C	-2.906267	-2.215894	-0.682130
C	-4.274278	-2.258184	-0.953823
C	-6.833457	-0.440822	-2.832452

C	-7.116288	-2.553733	-1.513416
C	7.887881	1.379919	-1.108344
O	-0.913476	-0.985532	-0.349498
V	0.347187	0.417385	0.123885
O	1.789309	-0.833936	-0.307973
C	3.633374	0.686844	-0.695072
C	3.072695	-0.614955	-0.425330
C	3.991494	-1.702307	-0.313244
C	5.362894	-1.505746	-0.436148
C	5.939070	-0.224536	-0.695724
C	5.047634	0.840574	-0.827981
C	2.802190	1.834901	-0.925355
N	1.497237	1.897891	-0.789812
C	7.469509	-0.076564	-0.820163
C	8.137193	-0.522869	0.506240
C	7.981471	-0.969762	-1.979528
C	-2.365762	1.527433	-0.748280
N	-1.113927	1.776457	-0.465417
H	9.084762	-0.887949	-2.075120
H	7.529346	-0.665236	-2.945934
H	7.739347	-2.039440	-1.815919
H	9.241959	-0.437269	0.433383
H	8.992180	1.445684	-1.189528
H	7.462016	1.751573	-2.063117
H	3.574249	-2.701033	-0.115461
H	5.420883	1.853230	-1.044017
H	6.022267	-2.382132	-0.327734
H	-6.981757	-3.084507	-0.548642
H	-6.630155	-3.155457	-2.308607
H	-4.755485	-3.245560	-1.006840
H	-2.330741	-3.141129	-0.529043
C	-0.734036	5.633259	-0.794620
C	-1.474542	4.288060	-0.899594
C	-0.567541	3.143868	-0.430072
C	0.590336	5.610181	-1.571457
C	1.497925	4.447925	-1.129223
C	0.755821	3.104771	-1.229835
H	3.338806	2.736792	-1.281783
H	0.476716	2.936296	-2.298179
H	0.377023	5.512038	-2.659487
H	-1.386289	6.450985	-1.165554
H	2.410938	4.440045	-1.759061
H	-1.785025	4.110635	-1.953901
O	0.413172	0.648686	1.705853